# Stirling Engine Technology and Its Application on Solar Power Generation

**Chin-Hsiang Cheng and Hang-Suin Yang**

**Abstract** In this study, a beta-type 500-W Stirling engine is developed and tested, and a nonideal adiabatic model is built and applied to predict performance of the engine. Engine torque, engine speed, and shaft power output are measured under various operating conditions. Furthermore, as the charged pressure and the heating temperature are set at eight bars and 800 °C and a No. 50 wire mesh is used in the regenerator, the shaft power of the engine can reach 556 W at 1665 rpm with 1.21-kW input heat transfer rate (45.95 % thermal efficiency). The experimental data are compared with the numerical predictions to verify the theoretical model. It is found that the experimental data of the shaft power output closely agree with the numerical predictions. This implies that the theoretical model is valid and helpful to the engine design.

**Keywords** Stirling engine · Solar power · Experiment · Numerical model

## 1 Introduction

Stirling engines are referred to as external combustion engines, and hence, they can be operated with a variety of heat sources and have been applied for energy conversion in a number of engineering applications. The ideal regenerative Stirling cycle consists of two isothermal processes and two isochoric processes. In theory, the thermal efficiency of an ideal regenerative Stirling cycle is equal to the Carnot cycle efficiency under the same thermal reservoirs temperatures. Due to the above advantages, Stirling engines have been used in concentrating solar power (CSP) systems that adopt mirrors or lenses to concentrate a large area of solar energy onto a

C.-H. Cheng (✉) · H.-S. Yang
Department of Aeronautics and Astronautics, National Cheng Kung University, No.1, Ta-Shieh Road, Tainan 70101, Taiwan, Republic of China
e-mail: chcheng@mail.ncku.edu.tw

R. P. Bajpai et al. (eds.), *Innovative Design, Analysis and Development Practices in Aerospace and Automotive Engineering*, Lecture Notes in Mechanical Engineering,
DOI: 10.1007/978-81-322-1871-5_1, © Springer India 2014

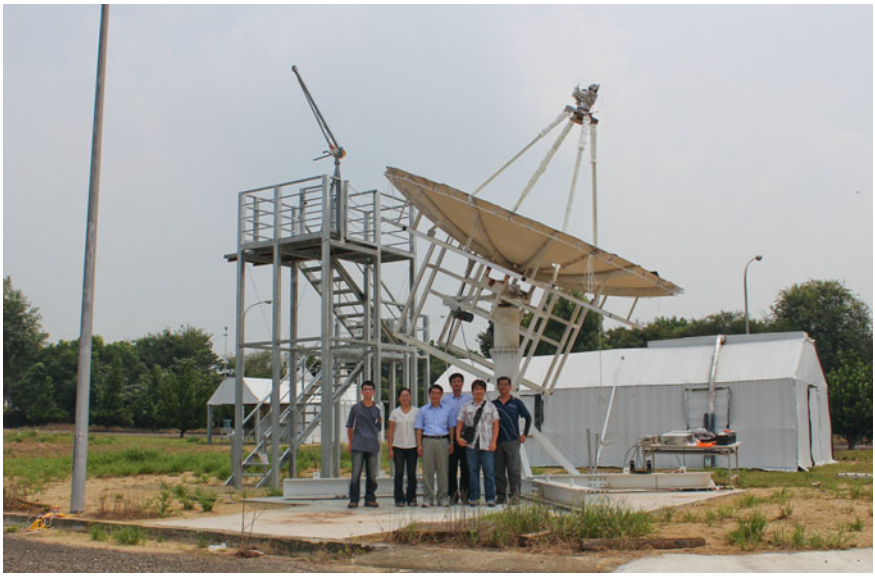

**Fig. 1** 20 kW-class concentrating solar power (CSP) systems. (Developed by Power Engines and Clean Energy Laboratory [PEACE Lab.], National Cheng Kung University)

small area. Figure 1 shows the CSP system developed by Department of Aeronautics and Astronautics, National Cheng Kung University. Electrical power is produced when the concentrated sunlight is converted to thermal energy to drive the Stirling engine and connected to an electrical power generator [1]. Since Stirling engine is suitable for various heat source, in addition to CSP systems, it is also suitable for variable external heat sources, including waste heat, geothermal energy, and combustion heat from fossil fuels or hydrogen provided that heating temperature of any external heat source is sufficiently high. Therefore, the Stirling engine technology receives increasing attention from energy-related researchers in recent years.

The first patent of the Stirling engine was filed by Robert Stirling in 1817 who originally intended to invent a hot-air closed-cycle prime mover to serve as an alternative to the explosively dangerous steam engine. In 1871, Schmidt proposed an isothermal second-order analysis of the ideal Stirling engine cycle. In order to modify this model, Finkelstein [2] presented ideal adiabatic models, in which the thermodynamic processes taking place in the expansion and the compression spaces are assumed to be adiabatic. However, the heater and the cooler are still assumed to be isothermal. In a real engine, the thermal conditions are not isothermal or adiabatic. Recently, Cheng et al. [3] developed a nonideal adiabatic model for a beta-type Stirling engine with rhombic-drive mechanism by introducing effectiveness of mechanism [4], effectiveness of regenerator, imperfect heat transfer, and pressure drop. Moreover, Cheng and Yang [5] establish a nondimensional thermodynamic model to optimize the geometry of rhombic-drive mechanism, and give an optimal design for maximum shaft work.

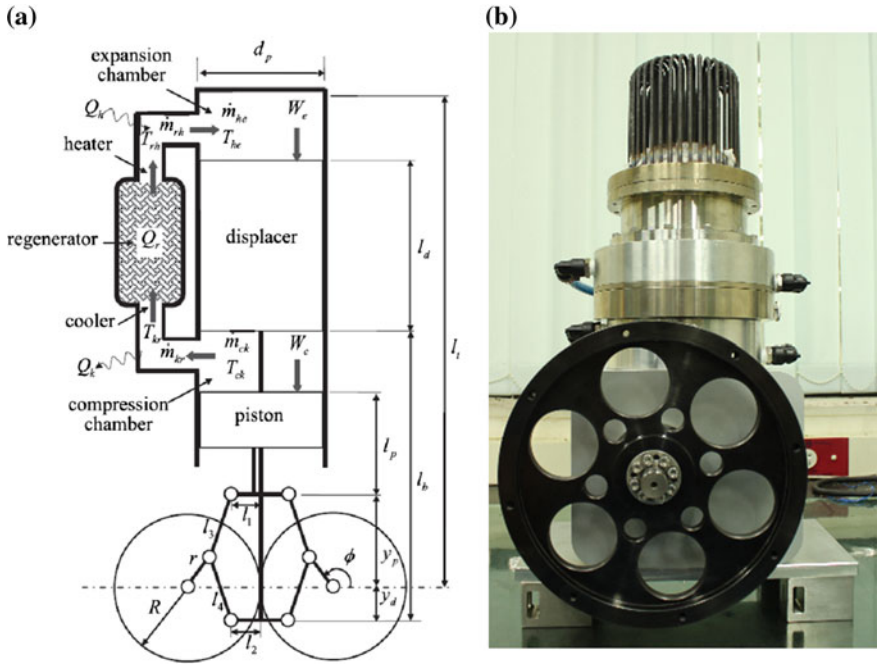


**Fig. 2** Schematic diagram and photo of prototype engine. **a** Schematic diagram, **b** Photographic copy

In general, Stirling engines can be divided into three major categories, namely, alpha-, beta-, and gamma-types. And the beta-type engine has higher power density than the other two types, as shown by Cheng and Yang [6]. Therefore, in this study, the beta-type Stirling engine with rhombic-drive mechanism is developed. Experiments are also conducted to test the performance of the engine under various operating conditions. In parallel, a theoretical model is built and applied to predict performance of the engine. Eventually, the obtained experimental data are compared with the numerical predictions to verify the theoretical model.

## 2 Engine Design

The schematic of the beta-type Stirling engine with rhombic drive mechanism and photo of the prototype engine are shown in Fig. 2. The rhombic drive, which is frequently used with the beta-type Stirling engines, utilizes a jointed rhomboid to convert linear motion of a reciprocating piston to a rotational of flywheel. In the rhombic drive mechanism, one rigid rod is installed connecting the piston to the top corner of the jointed rhomboid, and another rigid rod connecting the displacer to the bottom corner of the rhomboid. In addition, two symmetric gears of equal

**Table 1** Engine specifications

| | |
|---|---|
| Stroke | 35 mm |
| Bore size | 70 mm |
| Phase angle of volume | 105.537° |
| Swept volume ratio | 1 |
| Dead volume ratio | 1.478 |
| Compression ratio | 1.364 |
| Charged pressure | 8 atm |
| Working fluid | Helium |
| Heating temperature | 600–800 °C |
| Cooling temperature | 27 °C (liquid cooling) |

diameter are connected to the right and the left corners of the rhomboid fixed on the gears at an offset distance from gears center. The design parameters of the prototype engine are tabulated in Table 1.

## 3 Theoretical Model

In this study, a nonideal adiabatic model that involves the friction loss due to mechanism, power loss due to pressure drop, and the heat loss due to imperfect regeneration is proposed. The assumptions with the model are:

(1) The pressure is uniform throughout the interior space of the engine.
(2) The expansion chamber and the compression chamber are insulated.
(3) The heat is absorbed in the heater and rejected in the cooler.
(4) The temperature distribution in the regenerator is varied linearly from the heater's temperature to the cooler's temperature.
(5) The working gas is regarded as an ideal gas.

The detail process of nonideal adiabatic model is described in [3]. With the help of nonideal adiabatic model, indicated power and power loss due to friction loss can be calculated. However, mechanism loss has to be considered to obtain shaft power. The correlations of mechanism loss under different engine speed and heating temperature can be obtained by comparing the data which calculated by numerical model and measured by experiments. Generally, mechanism loss can be calculated by following formula.

$$\dot{W}_{m,loss} = A\omega^3 + B\omega^2 + C\omega + D \text{ (W)} \tag{1}$$

where $A$, $B$, $C$, and $D$ are function of heating temperature, and $\omega$ is engine speed.

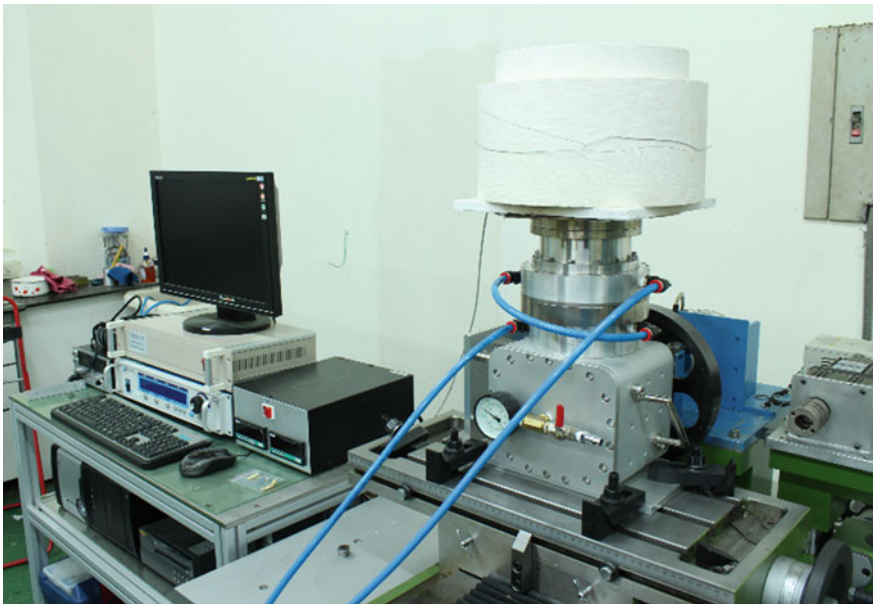

**Fig. 3** Experimental apparatus and measuring devices

## 4 Experimental Apparatus

The experimental apparatus for the engine performance test is shown in Fig. 3. An electric infrared heater of 1.21 kW (11 A/110 V) is used as the external heat source, and a thermostat is used to control the heating temperature. A K-type thermocouple is placed in the center of the electric infrared heater to monitor the heating temperature and the temperature data are recorded by a data logger. In experiments, the engine load is applied on the crank shaft of the engine by using a hysteresis brake dynamometer. The dynamometer provides brake torque loading independent of the engine speed. The rotation speed of the engine and the brake torque can be measured by a rotation meter and a torque sensor, respectively. The data are also recorded by the data logger. The shaft power is then determined in terms of the brake torque and the engine rotation speed.

## 5 Results and Discussion

In this section, effects of the mesh number of the regenerator and the heating temperature are measured experimentally and predicted theoretically. Figure 4 conveys the comparison between experimental and numerical data in the shaft power as a function of engine speed and mesh number. The symbols are

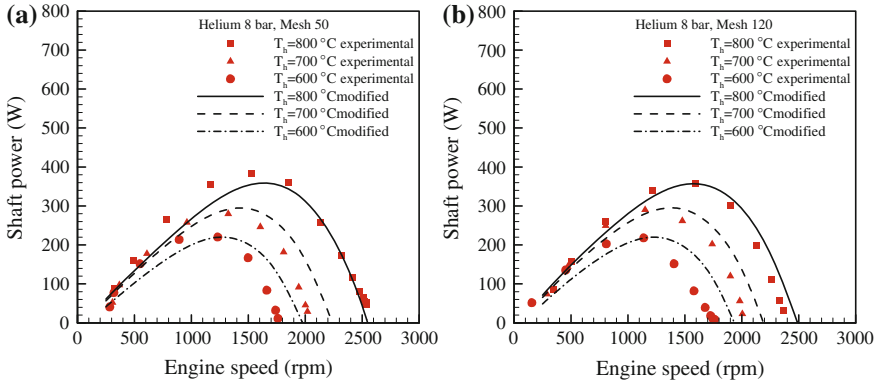


**Fig. 4** Experimental data and simulation results with different mesh number of regenerator. **a** 8 atm helium, No.50 **b** 8 atm helium, No.120

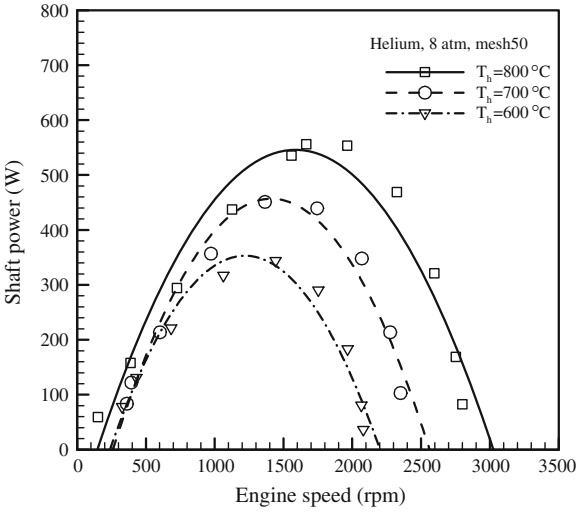


**Fig. 5** The experimental data with 8 atm helium, No.50 mesh, and enhanced cooling

experimental data and the lines are obtained from simulation result. The results reveal that the maximum shaft power output decreases as the mesh number is increased from No. 50 to No. 120. The corresponding maximum shaft power is 384 W at 1,530 rpm and 356 W at 1,595 rpm respectively. And the results also show that the simulation results in accordance with experiment data well, and the error is lower than 17%.

Furthermore, for the case of Fig. 4a, the maximum shaft power can reach about 556 W at 1,665 rpm as the cooling system is enhanced as Fig. 5 shows. With 1.21-kW input heat transfer rate, thermal efficiency can reach 45.95 %.

## 6 Conclusions

In this study, a domestic scale 550-W Stirling engine with rhombic-drive mechanism is developed and tested. The shaft power of the engine can reach 556 W at 1,665 rpm with 1.21-kW input heat transfer rate, which means a thermal efficiency of 45.95 %. The theoretical model is valid and helpful to the engine design, and the engine can be applied on CSP system.

**Acknowledgments** Financial supports from the National Science Council, Taiwan, under grant NSC 102-2221-E-006-088, and from the Southern Taiwan Science Park Administration (STSPA), Taiwan, under contract 101CP03, are greatly appreciated.

## References

1. Mancini T, Heller P, Butler B, Osborn B, Schiel W, Goldberg V, Buck R, Diver R, Andraka C, Moreno J (2003) Dish-stirling systems: an overview of development and status. J Sol Energy Eng, Trans ASME 125(2):135–151
2. Finkelstein T (1975) Computer analysis of stirling engines. Adv Cryog Eng 20:269–282
3. Cheng CH, Yang HS, Keong L (2013) Theoretical and experimental study of a 300-W beta-type stirling engine. Energy 59:590–599
4. Senft JR (2000) Extended mechanical efficiency theorems for engines and heat pumps. Int J Energy Res 24(8):679–693
5. Cheng CH, Yang HS (2014) Optimization of rhombic drive mechanism used in beta-type Stirling engine based on dimensionless analysis. Energy 64:970–978.
6. Cheng CH, Yang HS (2012) Optimization of geometrical parameters for Stirling engines based on theoretical analysis. Appl Energy 92:395–405